Indonesian Journal of Science & Technology

Journal homepage: http://ejournal.upi.edu/index.php/ijost/

Measurement and Quantitative Analysis of Ozone Generation in Radiation Treatment Room Due to High-Energy Photon

*Jung Keun Cho, Kyoungho Choi**

Jeonju University, Jeonju, Republic of Korea
*Correspondence: E-mail: ckh414@jj.ac.kr

ABSTRACT

Ozone generation in radiation treatment rooms poses a health risk due to high-energy photon interactions with air molecules. This study quantifies ozone concentration under varying conditions and assesses its impact on occupational exposure. Using a self-designed phantom, ozone measurements were taken under various conditions, including different photon energies (i.e., 6 and 15 MV), dose rates (i.e., 300 and 600 MU/min), and doses (i.e., 500 and 1,000 MU), with each condition measured ten times. Results showed that ozone concentration increased significantly with higher photon energy and dose, while the dose rate had a minimal effect, except at 15 MV. The highest ozone level (0.161 ± 0.003 ppm) exceeded FDA medical device limits and air quality standards. Ozone persisted for six minutes before normalizing, posing potential health risks to workers. These findings highlight the need for improved ventilation strategies in radiation treatment rooms.

ARTICLE INFO

Article History:
Submitted/Received 18 Jan 2025
First Revised 20 Feb 2025
Accepted 09 Apr 2025
First Available Online 10 Apr 2025
Publication Date 01 Sep 2025

Keyword:
Dose rate,
High energy photon,
Monitor unit,
Ozone produce,
Photon energy,
Radiation treatment room.

1. INTRODUCTION

Radiation therapy is one of the primary treatment modalities for cancer, alongside chemotherapy and surgery [1, 2]. While early radiation therapy utilized low-energy X-rays (~100 kV), modern treatments employ high-energy photons (> 6 MV) to improve dose distribution and penetration depth. However, high-energy photons can ionize oxygen molecules in the air, leading to the production of ozone (O_3), which may pose health risks in radiation treatment rooms.

Ozone is primarily generated through ionization by high-energy photons and secondary photochemical reactions involving nitrogen oxides (NOx) and volatile organic compounds (VOCs) [3, 4]. While ozone has beneficial applications in areas such as water purification and air disinfection [5], excessive exposure can have detrimental effects on respiratory health, even at low concentrations [6]. Regulatory agencies, including the U.S. Food and Drug Administration (FDA) and the Environmental Protection Agency (EPA), have established exposure limits for ozone, with medical devices restricted to 0.05 ppm and occupational exposure limits set at 0.1 ppm over 8 hours (OSHA) [7-9].

Despite the well-documented risks of ozone exposure, previous studies on ozone generation in radiation therapy rooms have been limited in scope. Most have focused on measuring ambient ozone levels without quantitatively analyzing the effects of different radiation parameters such as photon energy, dose, and dose rate. Unlike previous studies that only measured ambient ozone levels qualitatively, this research provides a quantitative assessment of ozone generation under controlled conditions, systematically analyzing the influence of photon energy, dose rate, and dose. Additionally, we introduce a self-designed phantom to ensure precise ozone measurements within an ionization volume, which has not been explored in prior studies. Our findings also highlight that at 15 MV and high dose conditions, ozone concentrations exceed FDA and national air quality standards, raising significant occupational safety concerns that have been previously underreported in radiation therapy settings.

Since ozone was first discovered in 1839 by a German chemist [10], followed by the development of an ozone generator in 1857 [11] and the first study on ozonide reactions in 1905 [12], its effects on human health have been widely studied. Research has shown that ozone can have fatal effects on cells, particularly in the respiratory system [13]. In recent years, to protect humans from ozone exposure, regulatory measures have been implemented, including ozone warnings at concentrations exceeding 0.12 ppm, ozone advisories at 0.3 ppm, and critical alarms at 0.5 ppm [14].

This study employed a systematic approach to quantitatively measure ozone generation in a radiation treatment room using a self-designed phantom and a high-precision gas detector (GAS TIGER 6000, Wandi, with an error margin of ±3% FS). Measurements were conducted under varying photon energy (i.e., 6 and 15 MV), dose rate (i.e., 300 and 600 MU/min), and dose (i.e., 500 and 1,000 MU) conditions, with each condition tested 10 times to ensure statistical reliability. Ozone concentrations were recorded using a detector positioned within a controlled chamber at a fixed source-chamber center distance (SCD) of 100 cm and a field size of 40×40 cm^2. The results were analyzed using IBM SPSS V25 for statistical significance. By systematically evaluating these parameters, this research not only quantifies ozone production under varying radiation conditions but also provides novel insights into how different radiation parameters affect ozone formation, which has been underreported in radiation oncology research. These findings offer essential data to improve occupational safety and regulatory compliance in radiation treatment environments.

DOI: https://doi.org/10.17509/ijost.v10i2.82093
p- ISSN 2528-1410 e- ISSN 2527-8045

2. METHODS

2.1. Measuring Equipment

For this experiment, we used a linear accelerator (Clinac IX, USA), a high-performance gas detector (GAS TIGER 6000, Wandi) with an ozone measurement error of ≤ ± 3% FS (Full scale), and a self-made chamber for quantitative analysis.

2.2. Measurement Method

To quantitatively analyze ozone generation by high-energy photons, a device in **Figure 1** was designed by placing a self-made chamber on the table of the linear accelerator and installing a high-performance gas detector inside to measure ozone generation within the ionization volume.

Radiation was irradiated under varying photon energy, dose, and dose rate conditions while maintaining a source-chamber center distance (SCD) of 100 cm and a field size of 40×40 cm^2. As shown in **Figure 1(a)**, the experimental setup consists of a linear accelerator, a self-designed phantom, and a gas detector positioned within the chamber. **Figure 1(b)** provides a magnified view of the gas detector inside the chamber, highlighting its placement for precise ozone measurement. The measured ozone concentration and its variations were continuously monitored using an observation camera installed in the treatment room.

(a) (b)

Figure 1. Equipment setting for measuring ozone generation by high-energy photons.

2.3. Measurement List

Table 1 presents the structured experimental design established to investigate how different radiation parameters—namely, photon energy, dose rate, and dose—affect ozone generation in a controlled radiation treatment room setting. A full factorial design was employed, incorporating two levels for each of the three variables: photon energy (i.e., 6 and 15 MV), dose rate (i.e., 300 and 600 MU/min), and dose (i.e., 500 and 1,000 MU). These conditions were selected based on their clinical relevance as they represent typical operational settings used in modern linear accelerators for both superficial and deep-tissue treatments. The field size was fixed at 40×40 cm^2, and the source-chamber center distance (SCD) was consistently maintained at 100 cm to ensure uniformity across all measurements. Each of the eight parameter combinations was measured ten times, providing a total of 80 data points. This repetition was critical to achieving statistical robustness, minimizing random errors, and allowing the use of parametric and non-parametric statistical analyses. Importantly, the chosen range of doses and energies allowed the study to evaluate not only the absolute generation of ozone but also the interaction effects between variables. For example, the higher photon energy (15 MV) was hypothesized to produce more ozone due to

DOI: https://doi.org/10.17509/ijost.v10i2.82093
p- ISSN 2528-1410 e- ISSN 2527-8045

increased ionization potential, which was confirmed in subsequent results. Similarly, the variation in dose rates was included to assess whether the rate of energy deposition, independent of total dose, would influence ozone formation. Overall, the experimental framework shown in **Table 1** served as the foundation for identifying critical thresholds in ozone production, which is essential for informing ventilation design and radiation safety protocols in clinical environments.

Table 1. Measurement conditions.

Field Size	Energy (MV)	Dose Rate (MU/min)	Dose (MU)
$40 \times 40\ cm^2$	6	300	500
			1000
		600	500
			1000
	15	300	500
			1000
		600	500
			1000

2.4. Measurement of Ozone Reduction over Time

The source-chamber center distance (SCD) was 100 cm, the field size was $40 \times 40\ cm^2$, and the energy was 15 MV, the dose rate was 600mu/min, and the dose was 1,000cGy. And time of decreasing from the maximum value of ozone produced under such conditions was measured 10 times, respectively.

2.5. Statistical Processing

IBM SPSS version 25 program was used, and Mann-Whitney's U test, a nonparametric two-sample independent test, was conducted to verify the change of ozone generation according to dose rate and dose. In addition, independent two-sample and Levene's equal variance tests were performed to verify the difference in ozone generation by energy.

3. RESULTS AND DISCUSSION

3.1. Results

3.1.1. Ozone generation by 6MV photons

Table 2 presents the quantitative measurements of ozone concentration obtained under four distinct combinations of dose and dose rate, using a photon energy of 6 MV. The experimental setup incorporated two dose rates (i.e., 300 and 600 MU/min) and two total doses (i.e., 500 and 1,000 MU), resulting in four unique test conditions. To ensure statistical robustness, each condition was measured ten times. The results demonstrate that ozone generation is strongly influenced by the total delivered dose. At a dose rate of 300 MU/min, the mean ozone concentration increased from 0.039 ± 0.003 ppm at 500 MU to 0.111 ± 0.006 ppm at 1,000 MU. A similar trend was observed at 600 MU/min, where ozone levels rose from 0.040 ± 0.005 ppm to 0.143 ± 0.005 ppm as the dose doubled. Although minor differences were observed between the two dose rates at equivalent dose levels, the variations were relatively small, suggesting that the dose rate has a limited impact on ozone formation at 6 MV. The low standard deviations across all measurements indicate high consistency and repeatability, reinforcing the reliability of the data. These findings imply that at a constant beam energy, ozone generation is primarily governed by the total number of ionizing events (i.e., the dose), rather than the speed at which they are delivered (i.e., the dose rate).

DOI: https://doi.org/10.17509/ijost.v10i2.82093
p- ISSN 2528-1410 e- ISSN 2527-8045

Therefore, this table also provides compelling evidence that at 6 MV, the radiation dose is the dominant factor in ozone production. This supports the hypothesis that greater cumulative energy deposition results in a higher yield of ionized oxygen molecules, thereby increasing ozone formation. These insights are essential for informing the development of dose-dependent safety guidelines in clinical radiation therapy settings.

Figure 2 provides a visual representation of the ozone concentration data obtained from irradiation with 6 MV photon beams, as summarized in **Table 2**. The figure demonstrates the dose-dependent nature of ozone generation. Both at 300 and 600 MU/min, ozone concentrations increase in a near-linear fashion as the dose rises from 500 to 1,000 MU. The slope of the increase is steeper for the higher dose rate (600 MU/min), but the overall pattern indicates that the primary driver of ozone production is the total delivered dose, not the speed of delivery. The visualization enhances the interpretability of the data by making trends and comparisons more immediately apparent than tabular data alone. For example, one can observe that the increase in ozone concentration from 500 to 1,000 MU is more substantial at the higher dose rate, even if the difference in absolute values is not dramatic. This suggests a possible secondary effect of dose rate, though less influential than the dose itself. Moreover, the graphical format allows for easier identification of linear or nonlinear trends, potential thresholds, or saturation effects, which are critical when extrapolating findings to real-world clinical settings. In addition, **Figure 2** helps confirm the consistency of measurement data across repetitions, as the error bars (standard deviations) are small, indicating tight clustering of results. This further strengthens confidence in the experimental methodology. From a clinical perspective, the figure underscores that significant ozone levels may be generated even at standard treatment energies like 6 MV, particularly as treatment doses increase. Thus, the figure serves as a compelling visual tool to support the study's conclusion that radiation dose is the dominant factor in ozone generation during therapeutic photon beam exposure.

Table 2. Ozone generation irradiated with various parameters.

Field Size	Energy	Dose Rate	Dose (MU)	O^3 (ppm)
$40 * 40cm^2$	6 MV	300 MU/min	500	0.039 ± 0.003
			1000	0.111 ± 0.006
		600 MU/min	500	0.04 ± 0.005
			1000	0.143 ± 0.005

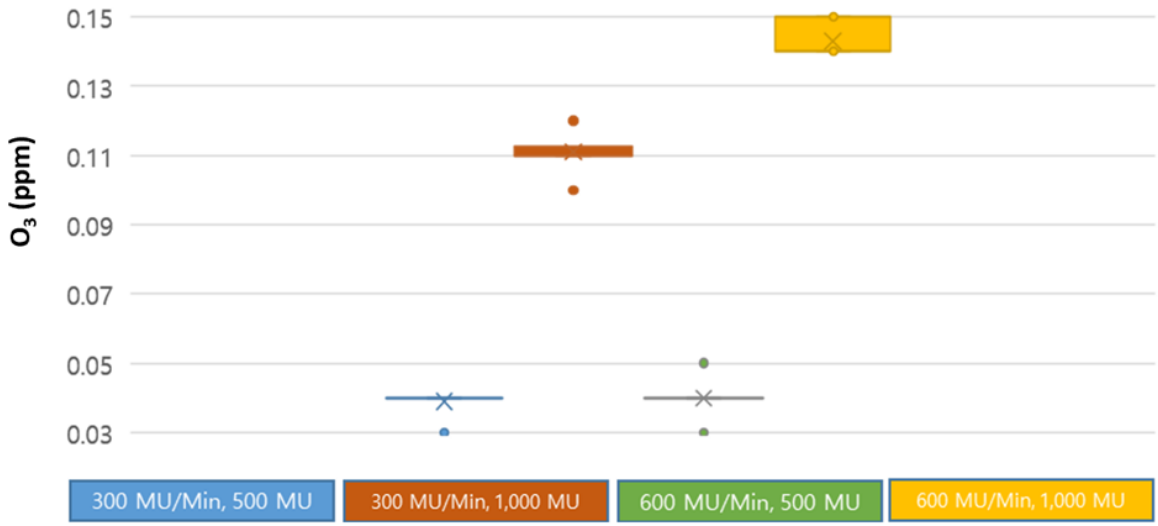

Figure 2. Ozone generated by 6 MV photons.

DOI: https://doi.org/10.17509/ijost.v10i2.82093
p- ISSN 2528-1410 e- ISSN 2527-8045

3.1.2. Ozone generation by 15MV photons

Table 3 displays the measured ozone concentrations under four different conditions using a photon energy of 15 MV. The dose rates of 300 and 600 MU/min were each combined with two dose levels: 500 and 1,000 MU. As with previous measurements, each condition was repeated ten times to ensure statistical robustness. The results demonstrate a consistent and substantial increase in ozone concentration with increasing dose, reinforcing the dose-dependent behavior observed in the 6 MV experiments. Specifically, at a dose rate of 300 MU/min, ozone concentration increased from 0.052±0.004 ppm at 500 MU to 0.142±0.004 ppm at 1,000 MU. Similarly, at 600 MU/min, values increased from 0.081±0.006 ppm to 0.161±0.003 ppm. Compared to the 6 MV results in **Table 2**, **Table 3** indicates that 15 MV photons consistently produce more ozone under equivalent dose and dose rate conditions. For instance, at 1,000 MU and 600 MU/min, ozone concentration was 0.161 ppm at 15 MV versus 0.143 ppm at 6 MV. This difference is likely due to the higher ionization efficiency of 15 MV beams, which generate more secondary electrons and enhance air molecule dissociation. The relatively small standard deviations again suggest high measurement reliability. These findings confirm that both dose and photon energy significantly influence ozone production. Interestingly, the increase in ozone between dose rates is slightly more pronounced at 15 MV, suggesting that the dose rate may exert a more meaningful effect at higher energies, a trend supported by statistical tests in **Table 4**. **Table 3** thus provides strong empirical evidence that ozone production intensifies with both increasing energy and dose, highlighting potential safety concerns in high-energy radiation treatment environments.

Table 3. Ozone generation irradiated with several processing parameters.

Field Size	Energy	Dose Rate (MU/min)	Dose (MU)	O_3 (ppm)
$40 \times 40\ cm^2$	15 MV	300	500	0.052±0.004
			1000	0.142±0.004
		600	500	0.081±0.006
			1000	0.161±0.003

Figure 3 offers a graphical representation of the ozone generation data measured with 15 MV photon beams, as summarized in **Table 3**. This figure visually reinforces the dose-dependent increase in ozone concentration observed in the data. Notably, compared to the patterns shown in **Figure 2** (6 MV), the increase in ozone levels at 15 MV appears both steeper and more pronounced across all dose and dose rate combinations. At both 300 and 600 MU/min, the progression from 500 to 1,000 MU shows a near-linear trend, but the slope of the line is higher than in the 6 MV case, reflecting the stronger ionization power of 15 MV photons. The graphical format also allows us to observe the dose rate effect more clearly. At 15 and 1,000 MU, the ozone concentration is 0.142 ppm at 300 MU/min and increases further to 0.161 ppm at 600 MU/min. This suggests that, at higher energies, the dose rate begins to play a more meaningful role in ozone formation, likely due to the increased rate of energy deposition within the same time interval. The figure also shows minimal variation between repetitions, as evidenced by the small error bars, indicating high precision and reliability in the measurement setup. From a safety and clinical operations standpoint, **Figure 3** underscores the potential for significant ozone accumulation during high-energy photon therapy, particularly when high doses and faster delivery rates are used. The figure thus serves as a compelling visualization of how energy and dose synergistically contribute to ozone production. These visual insights provide a foundation for assessing ventilation

DOI: https://doi.org/10.17509/ijost.v10i2.82093
p- ISSN 2528-1410 e- ISSN 2527-8045

requirements and refining occupational safety protocols in treatment facilities using 15 MV beams.

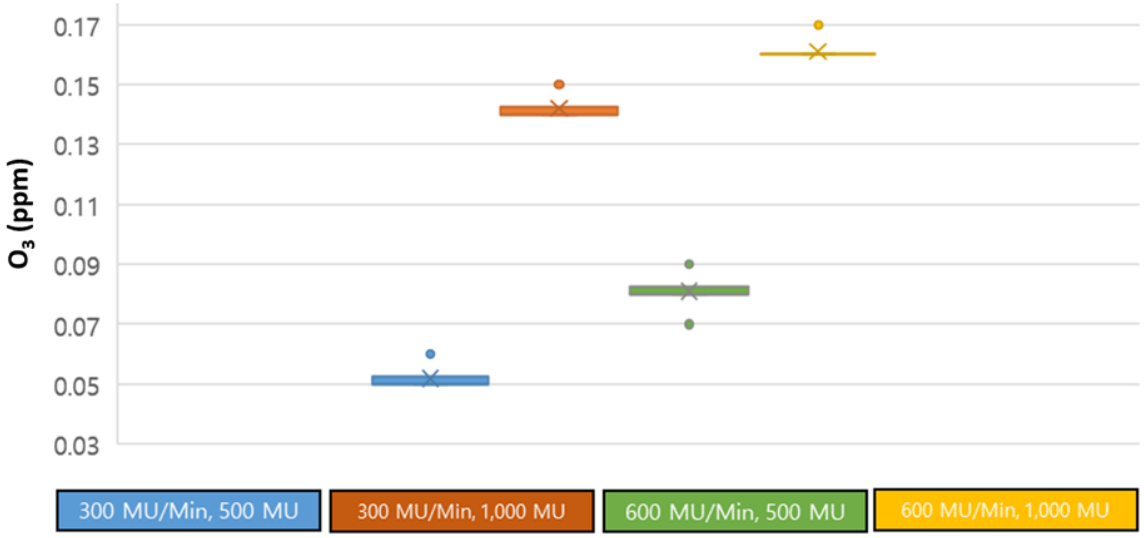

Figure 3. Ozone generated by 15 MV photons.

3.1.3. Ozone reduction over time

To assess the persistence of ozone after high-energy photon irradiation, an experiment was conducted to measure the rate of ozone reduction over time under specific conditions. The irradiation was performed using a photon energy of 15 MV, a dose rate of 600 MU/min, and a total dose of 1,000 MU, which corresponds to the condition that previously produced the highest ozone concentration in this study (0.161±0.003 ppm). Immediately after irradiation, ozone levels were continuously monitored to evaluate the decay characteristics within the closed chamber environment. As depicted in **Figure 4**, the decrease in ozone concentration followed a relatively consistent and linear trend over time, rather than an exponential decay pattern typically associated with gas dispersion in open environments. The half-life (defined as the time required for ozone concentration to drop to 50% of its peak value) was observed to be approximately 3 minutes. Complete normalization, or return to baseline levels, occurred around 6 minutes post-irradiation. This indicates that in the absence of ventilation or forced air exchange, residual ozone remains in the environment for a significant period after beam delivery has ceased. Given the potential respiratory effects of ozone, even at low concentrations, this delay in dissipation poses a risk to radiation workers who may enter the treatment room shortly after a high-dose procedure. The linear pattern of reduction suggests that ozone decay within this confined volume is primarily influenced by natural recombination and wall absorption processes rather than turbulent airflow. These findings support the need for implementing time-delayed room access and/or enhanced ventilation protocols in clinical settings where high-energy photon beams are routinely used.

3.1.4. Statistical analysis

Table 4 presents the results of statistical analyses conducted to verify the effects of photon energy, dose, and dose rate on ozone generation. A comparison of ozone concentrations between the two photon energies (i.e., 6 and 15 MV) revealed that higher photon energy resulted in significantly increased ozone production. The independent two-sample t-test confirmed this finding with a p-value of 0.013, indicating a statistically significant difference in ozone concentration depending on the photon energy level. Furthermore, the mean ozone

DOI: https://doi.org/10.17509/ijost.v10i2.82093
p- ISSN 2528-1410 e- ISSN 2527-8045

concentrations were compared according to delivered dose levels (i.e., 500 and 1,000 MU) at both dose rates (i.e., 300 and 600 MU/min). In all conditions, a highly significant difference was observed ($p < 0.001$), confirming that higher dose levels consistently led to elevated ozone concentrations, regardless of energy or dose rate. This highlights the dose-dependent nature of ozone formation during photon beam irradiation. In contrast, when the influence of the dose rate was analyzed independently for each photon energy level, the results were mixed. For 6 MV photons, the effect of dose rate on ozone generation was not statistically significant ($p = 0.142$), suggesting that ozone concentration at this energy is relatively insensitive to the rate of dose delivery. However, for 15 MV photons, a significant difference was found between the two dose rates ($p = 0.006$), indicating a dose rate effect at higher photon energies. To confirm the validity of the t-test results, Levene's test for equality of variances was conducted and satisfied ($p = 0.662$). The final t-test result ($t = -2.531$, $p = 0.013$) supported the conclusion that the mean ozone concentrations differ significantly by energy. These comprehensive statistical findings confirm that both photon energy and dose are primary contributors to ozone generation, while dose rate becomes a meaningful factor only at higher energies, providing a nuanced understanding of clinical radiation safety protocols.

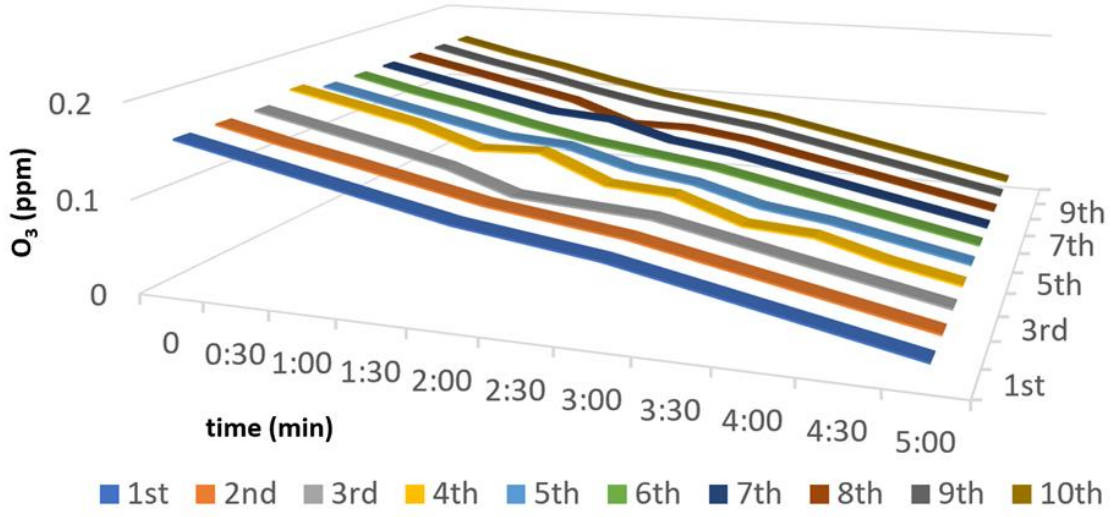

Figure 4. Change of ozone reduction over time.

Table 4. Significance test results according to energy, dose rate, and dose.

6 MV				15 MV			
300 MU/min	p=0.142	500 MU 1,000 MU	p<0.001	300 MU/min	P=0.006	500 MU 1,000 MU	p<0.001
600 MU/min		500 MU 1,000 MU	p<0.001	600 MU/min		500 MU 1,000 MU	p<0.001

Energy	p value
6 MV	p<0.013
15 MV	

3.2. Discussion

High-energy photon beams employed in modern radiotherapy can ionize atmospheric oxygen, leading to the formation of ozone (O_3)—a secondary pollutant known to pose respiratory health risks [6, 7]. This study aimed to quantify ozone production within a

DOI: https://doi.org/10.17509/ijost.v10i2.82093
p- ISSN 2528-1410 e- ISSN 2527-8045

controlled radiation environment and to investigate how photon energy, dose, and dose rate influence ozone concentration. As shown in **Tables 2, 3, and 4** and **Figures 2, 3, and 4**, both photon energy and total dose significantly impact ozone generation, aligning with previous findings on radiolytic gas production [15]. Notably, **Table 4** reveals a statistically significant effect of photon energy on ozone concentration ($p = 0.013$), while total dose consistently exerts a strong influence across all energy levels ($p < 0.001$). These results corroborate the findings of previous studies [3], which highlighted the role of ionizing radiation in enhancing oxidative reactions in the air. In contrast, the dose rate was only statistically significant at 15 MV ($p = 0.006$), indicating a possible threshold effect, potentially attributable to cumulative ionization density. **Figures 2 and 3** further illustrate these patterns, with ozone concentrations peaking at 0.143 ppm (6 MV) and 0.161 ppm (15 MV) when 1,000 monitor units (MU) were delivered.

Figure 5 presents a schematic of the experimental setup designed to measure ozone formation in a high-energy photon field. At the core of this system is a custom-designed phantom chamber, constructed to replicate the ionization volume where photon–air interactions predominantly occur. The phantom was engineered with a precisely calculated internal volume of 0.02 m^3 (20,000 cm^3), ensuring accuracy and reproducibility in ozone measurements. By limiting the sampling area to this defined volume, the setup overcomes a key limitation of previous studies that relied on ambient room measurements without spatial control [15]. The gas detector (GAS TIGER 6000) was positioned at the center of the phantom's irradiation volume, allowing it to capture ozone generated directly by the beam, isolated from external interferences. This configuration minimized confounding factors such as airflow variability, heterogeneous volatile organic compound (VOC) distributions, or reflective surfaces within the treatment room. The fixed distance from the source to the chamber center (100 cm) and a consistent field size of 40×40 cm^2 provided uniform irradiation, closely simulating clinical conditions. This phantom system represents a methodological advancement, enabling volumetric rather than point-based ozone quantification, thereby enhancing the spatial validity of the results. Such precision is critical not only for comparing experimental variables (e.g., dose and energy) but also for extrapolating the data to real-world scenarios. For example, this setup facilitates the scaling of ozone concentrations to room-sized environments, providing valuable input for ventilation design and occupational exposure risk assessments. This figure also reflects a key innovation of this study and offers a model for future evaluations of radiological environments.

Figure 4 illustrates the temporal behavior of ozone following irradiation. A half-life of approximately 3 minutes and complete dissipation within 6 minutes suggest that without adequate ventilation, residual ozone may linger long enough to pose a risk to healthcare personnel. These observations are consistent with the findings of previous studies [6], who reported that even brief exposures to concentrations as low as 0.1 ppm can negatively affect lung function. Given that the peak ozone concentrations measured in this study reached up to 0.161 ppm (surpassing both FDA and EPA thresholds of 0.05 and 0.1 ppm, respectively [8, 9], there is an urgent need to reassess and enhance ventilation protocols in treatment rooms. The results underscore the potential for ozone accumulation in environments utilizing high-energy photon beams and support the implementation of engineering controls or scheduling modifications to limit occupational exposure. Future research should build upon these findings by exploring the influence of clinical room geometries, ventilation system designs, and cumulative exposure over time.

DOI: https://doi.org/10.17509/ijost.v10i2.82093
p- ISSN 2528-1410 e- ISSN 2527-8045

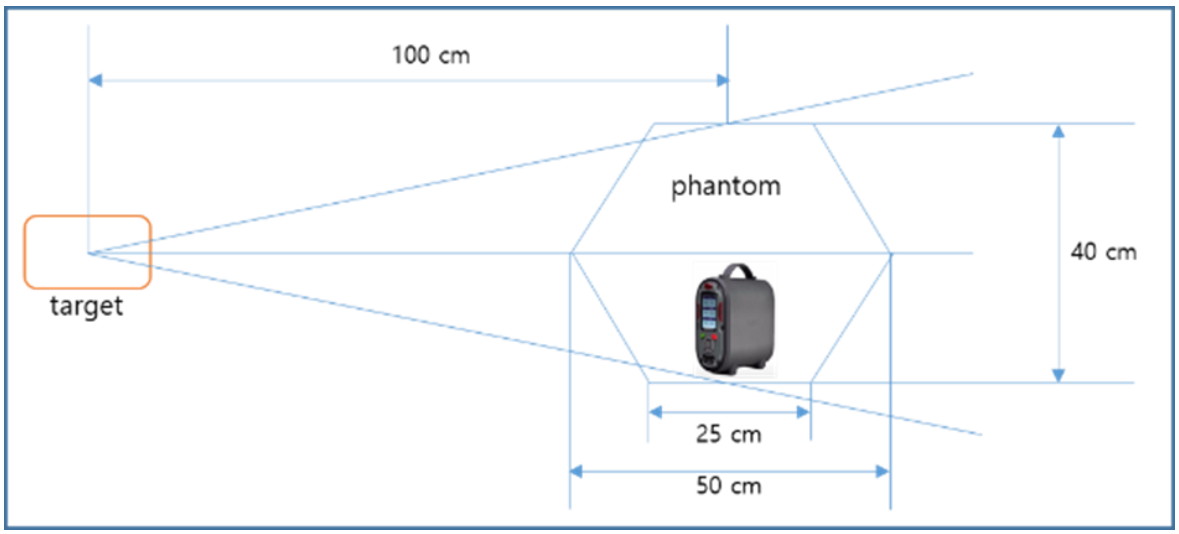

Figure 5. Schematic diagram of equipment setting (Results of ionization volume calculation in phantom (size of 0.02 m^3 or 20,000 cm^3).

4. CONCLUSION

This study quantitatively evaluated ozone generation in a radiation treatment room due to high-energy photons by varying energy, dose rate, and dose. Using a self-designed phantom, we systematically measured ozone concentration changes and identified key influencing factors. Our main results demonstrate the following: First, higher photon energy and dose significantly increase ozone concentration ($P < 0.001$). Second, the dose rate had a minimal impact at 6 MV ($P = 0.142$), but a significant difference was observed at 15 MV ($P = 0.006$). Third, ozone concentrations at 15 MV, 600 MU/min, and 1,000 MU (0.161±0.003 ppm) exceeded FDA and national air quality standards. Fourth, the ozone took approximately 6 minutes to return to normal levels, posing a potential health risk to radiation workers. These findings highlight the necessity of improved ventilation systems in radiation treatment rooms to mitigate occupational exposure risks. The study provides quantitative data for regulatory compliance and safety improvements in clinical settings.

While this study provides critical insights, it has the following limitations: First, measurements were conducted in a controlled environment using a self-designed phantom, which may not fully replicate real-world clinical conditions. Second, other factors influencing ozone generation, such as room size variations and additional radiation parameters, require further investigation. Third, volatile organic compounds (VOCs) produced by high-energy photons were identified, but their detailed effects were not analyzed. Future studies should expand the scope to larger-scale clinical environments, investigate long-term exposure effects, and explore advanced air purification solutions to reduce ozone accumulation in treatment rooms.

5. AUTHORS' NOTE

The authors declare that there is no conflict of interest regarding the publication of this article. The authors confirmed that the paper was free of plagiarism.

6. REFERENCES

[1] Yang, P., Xu, T., Gomez, D. R., Deng, W., Wei, X., Elhalawani, H., Jin, H., Guan, F., Mirkovic, D., Xu, Y., Mohan, R., and Liao, Z. (2019). Patterns of local-regional failure after intensity

DOI: https://doi.org/10.17509/ijost.v10i2.82093
p- ISSN 2528-1410 e- ISSN 2527-8045

modulated radiation therapy or passive scattering proton therapy with concurrent chemotherapy for non-small cell lung cancer. *International Journal of Radiation Oncology, Biology, Physics*, *103*(1), 123-131.

[2] Kharofa, J., Mierzwa, M., Olowokure, O., Sussman, J., Latif, T., Gupta, A., Xie, C., Patel, S., Esslinger, H., Mcgill, B., Wolf, E., and Ahmad, S. A. (2019). Pattern of marginal local failure in a phase II trial of neoadjuvant chemotherapy and stereotactic body radiation therapy for resectable and borderline resectable pancreas cancer. *American Journal of Clinical Oncology*, *42*(3), 247-252.

[3] Liu, Q., Liu, T., Chen, Y., Xu, J., Gao, W., Zhang, H., and Yao, Y. (2019). Effects of aerosols on the surface ozone generation via a study of the interaction of ozone and its precursors during the summer in Shanghai, China. *Science of the Total Environment*, *675*, 235-246.

[4] Cramariuc, R., Velisar, I., Milevschi, V., and Munteanu, V. (1998). New considerations of ozone generation and the influence of NO~x in ozone production and water treatment. *NATO Science Series 2: Environment Security, 63*, *313-340*.

[5] Botta, C., Ferrocino, I., Cavallero, M. C., Riva, S., Giordano, M., and Cololin, L. (2018). Potentially active spoilage bacteria community during the storage of vacuum packaged beefsteaks treated with aqueous ozone and electrolysed water. *International Journal of Food Microbiology*, *266*, 337–345.

[6] McDonnell, W. F., Stewart, P. W., and Smith, M. V. (2010). Prediction of ozone-induced lung function responses in humans. *Journal of the Inhalation Toxicology*, *22*(2), 160-168.

[7] Bennett, W. D., Hazucha, M. J., Folinsbee, L. J., Bromberg, P.A., Kissling, G. E., and London, S. J. (2007). Acute pulmonary function response to ozone in young adults as a function of body mass index. *Journal of the Inhalation Toxicology*, *19*(14), 1147-1154.

[8] Adams, W. C. (2002). Comparison of chamber and face-mask 6.6-hour exposures to ozone on pulmonary function and symptoms responses. *Journal of the Inhalation Toxicology*, *14*(7), 745-764.

[9] Schultheis, A. H., Bassett, D. J., and Fryer, A. D. (1994). Ozone-induced airway hyper responsiveness and loss of neuronal M2 muscarinic receptor function. *Journal of Applied Physiology*, *76*(3), 1088-1097.

[10] Pavelin, E.G, Johnson, C.E, Rughooputh, S, and Toumi, R. (1999). Evaluation of pre-industrial surface ozone measurements made using Schonbein's method. *Atmospheric Environment*, *33*(6), 919.

[11] Chung, H. K., Bellamy, H. S., and Dasgupta, P. K. (1992). Determination of aqueous ozone for potable water treatment applications by chemiluminescence flow-injection analysis. A feasibility study, *Talanta*, *39*(6), 593-598.

[12] McCully, K. S. (2019). Homocysteine, thioretinaco ozonide, and oxidative phosphorylation in cancer and aging: A proposed clinical trial protocol. *Methods in Molecular Biology*, *1866*, 285-310.

[13] Francis, M., Groves, A. M., Sun, R., Cervelli, J. A., Choi, H., Laskin, J. D., and Laskin, D. L. (2017). Editor's highlight: CCR2 regulates inflammatory cell accumulation in the lung and tissue injury following ozone exposure. *Toxicological Sciences*, *155*(2), 474-484.

DOI: https://doi.org/10.17509/ijost.v10i2.82093
p- ISSN 2528-1410 e- ISSN 2527-8045

[14] Kim, W. S. (2014). Citizen's health impact and countermeasures of high concentration ozone. *The Seoul Institute Policy Report*, *171*, 1-20.

[15] Kwak, Y. K., Yoon, I. K., Lee, J. H., Yoo, S. H. (2009). Consideration about ozone generation in the treatment room while treating a patient. *The Journal of Korean Society for Radiation Therapy, 21*(2), 75-82.

DOI: https://doi.org/10.17509/ijost.v10i2.82093
p- ISSN 2528-1410 e- ISSN 2527-8045